Electronic Supplementary Material (ESI) for Journal of Materials Chemistry A.

Long-term cycling stability of SnS_2-based Covalent Organic Nanosheet anode for Lithium-ion Batteries

Jeong-Hun Jang, [a] *Minseop Lee,* [a] *,Soohyeon Park,* [b] *Jae-Min Oh,* [c]* *Jin Kuen Park* [b]* *and Seung-Min Paek* [a]*

[a]Department of Chemistry, Kyungpook National University, Daegu 41566, Republic of Korea E-mail: smpaek@knu.ac.kr

[b]Department of Chemistry, Hankuk University of Foreign Studies, Yongin 17035, Republic of Korea, E-mail: jinpark@hufs.ac.kr

[c]Department of Energy and Materials Engineering, Dongguk University-Seoul, Seoul 04620, Republic of Korea. Email: jaemin.oh@dongguk.edu

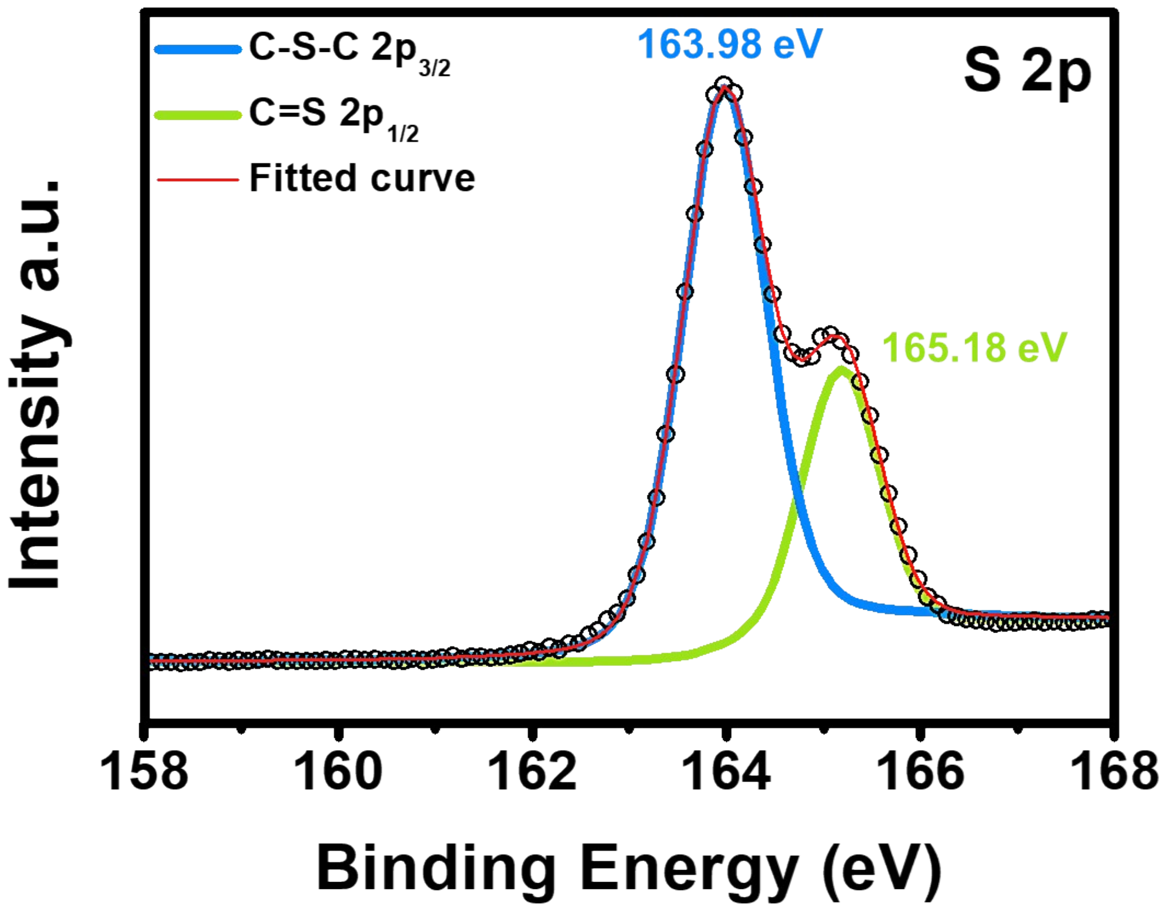

Figure S1. High-resolution S 2p XPS spectrum of CON-10.

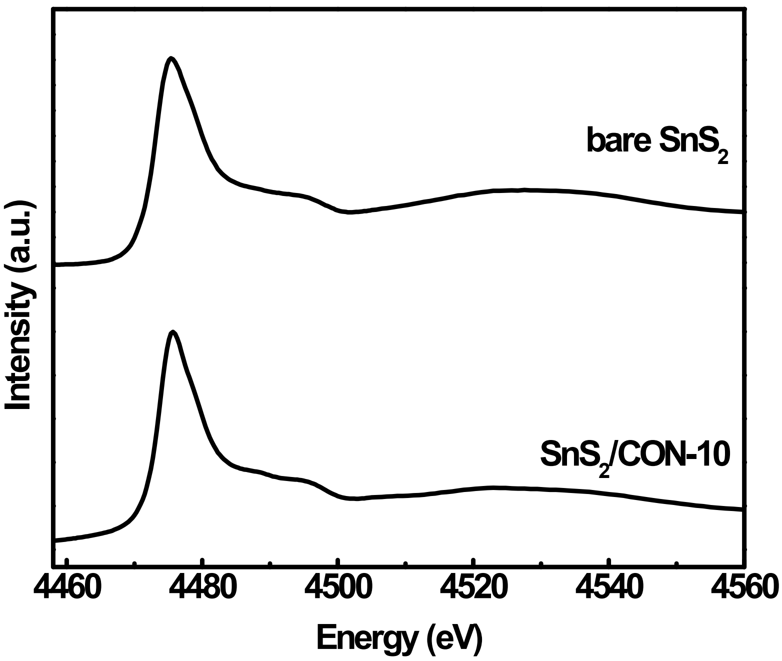

Figure S2. X-ray absorption near edge structure (XANES) data for bare SnS_2 and SnS_2/CON-10.

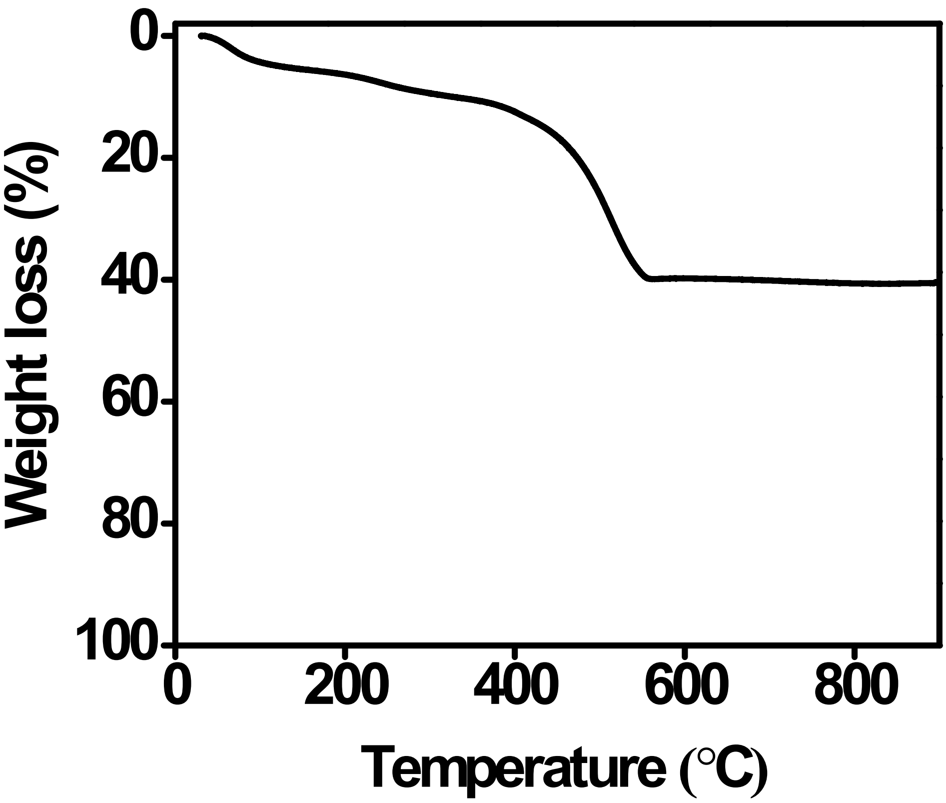

Figure S3. TGA curve of SnS_2/CON-10.

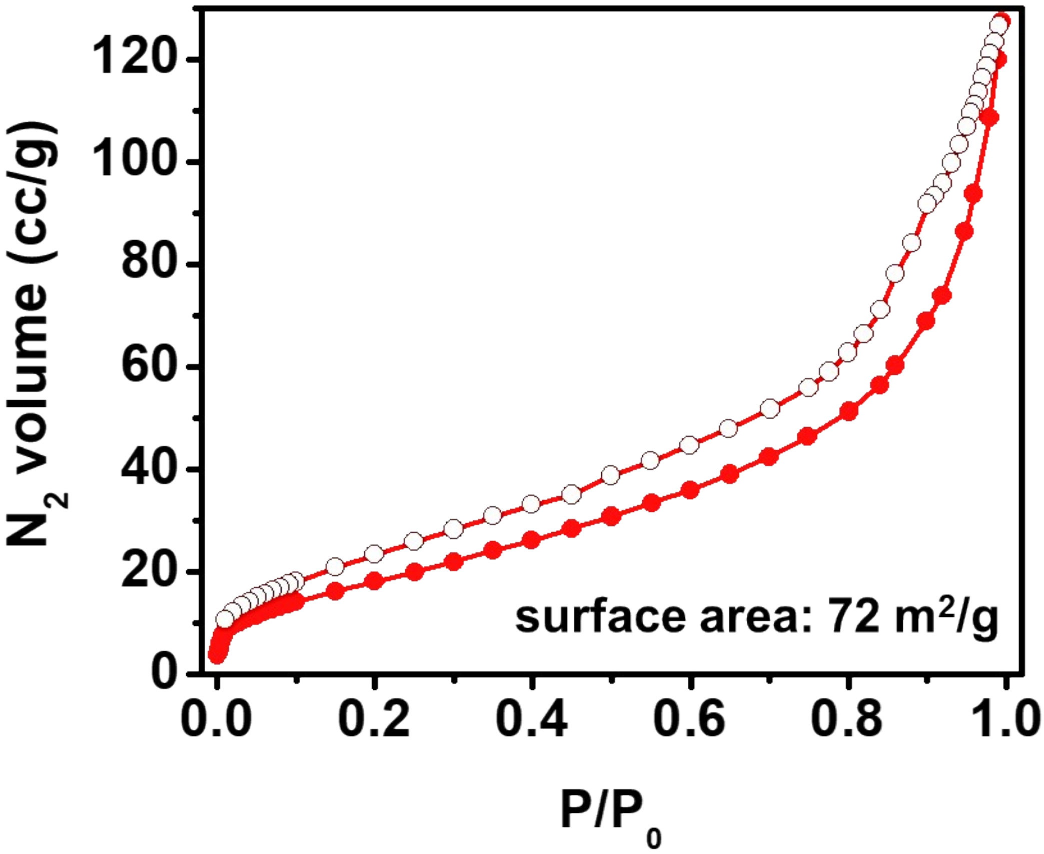

Figure S4. N_2 adsorption/desorption isotherm of SnS_2/CON-10.

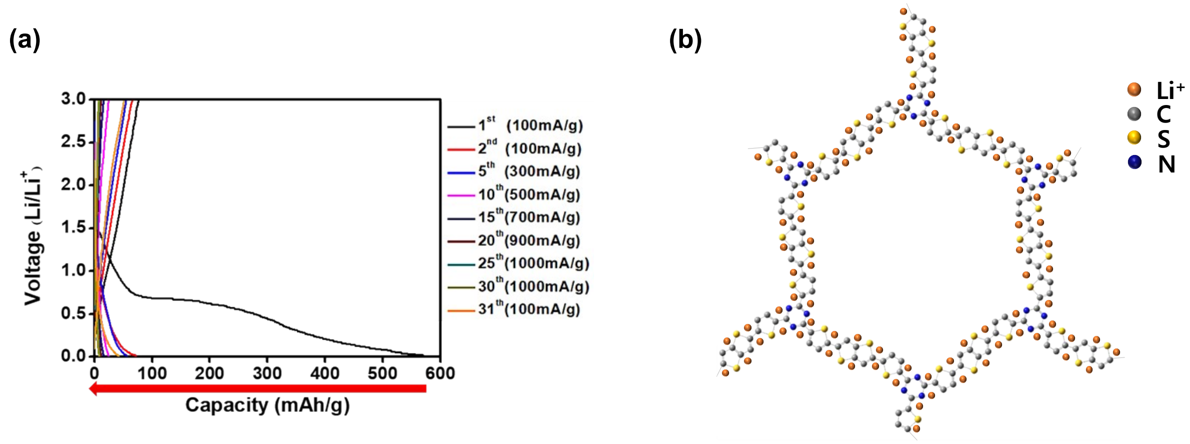

Figure S5. (a) Charge-discharge profile of CON-10 at 100 mA/g; (b) Schematic redox reaction mechanism of CON-10.

According to the previous literature,[1a] the reaction equation for SnS_2 via two steps (conversion/reconversion and alloying/dealloying) can be written as follows:

$$SnS_2 + 4Li^+ + 4e^- \rightarrow Sn + 2Li_2S$$

$$Sn + \chi Li^+ + \chi e^- \leftrightarrow Li_\chi Sn \ (0 \leq \chi \leq 4.4)$$

Theoretical Li-ion storage of CON-10 was calculated by Faraday's law equation as follows:

$$\text{Theoretical capacity (mAh/g)} = (n \cdot F)/(3600 \cdot M_w) \cdot 1000$$

Where n is the number of Li-ion, F is the Faraday constant (96485.3321 C/mol), and M_w is the molecular weight of the active materials. The repeating unit of CON-10 consists of two triazine, six thiophene, and three thionothiophene units where redox active sites are located on double-bond groups (C=C and C=N). We estimated that 30 Li^+ ions can be stored at a CON-10 repeating unit as seen in Figure S5(b).[1b] The molecular weight of the CON-10 repeating unit ($C_{48}N_6S_{12}H_{24}$) is calculated to be 1070 g/mol. From Faraday's law equation, the theoretical capacity of CON-10 was calculated to be 676 mAh/g, which is in good agreement with the discharge capacity of 1st cycle. Therefore the reaction equation for 1st cycle can be as follows:

$$C_{48}N_6S_{12}H_{24} + 27Li^+ + 27e^- \rightarrow Li_{27}C_{48}N_6S_{12}H_{24}$$

CON-10 loses most of its Li-ion storage capacity due to Li-ions being irreversibly trapped after the first discharge in Li-ion-accessible pores. On the other hand, in SnS_2/CON-10, SnS_2 generated at the pore part of CON-10 reduces the total pore volume (**Figure S4**).[1c] Therefore, SnS_2/CON-10 shows excellent capacity retention due to the synergistic effect of SnS_2 located in the pores of CON-10, where Li-ions were irreversibly captured, and CON-10, which prevents pulverization of SnS_2 (**Figure 8**).

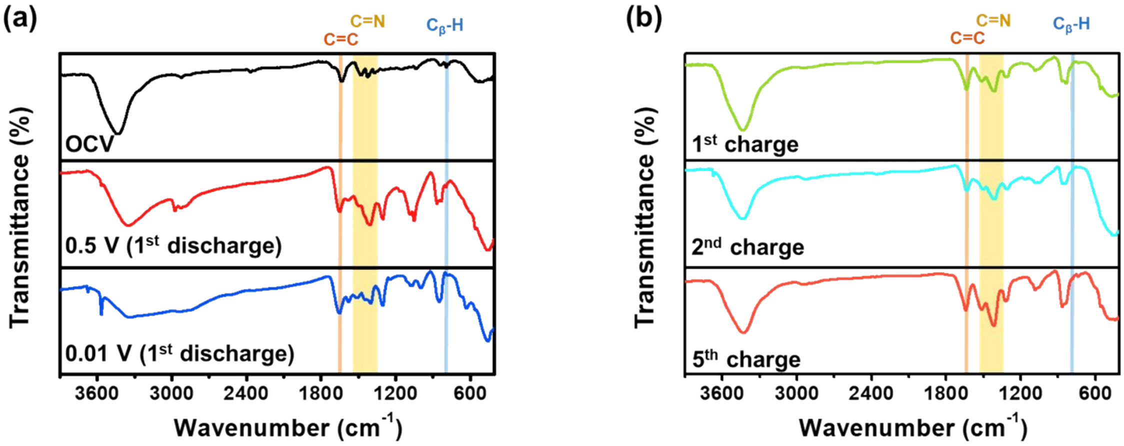

Figure S6. Ex-situ FTIR profiles of SnS_2/CON-10 electrodes upon varying voltages in the initial 5 cycles.

Although some irreversible electrolyte byproduct formation was observed after the 1st discharge cycle, the C=C vibration mode and the C=N stretching vibration peak of the CON-10 framework were well observed until the 5th cycle. Therefore, by comparing the FTIR profile of CON-10 reported in previous literature, it was confirmed that the structure of CON-10 inside the SnS_2/CON-10 electrode was well maintained.

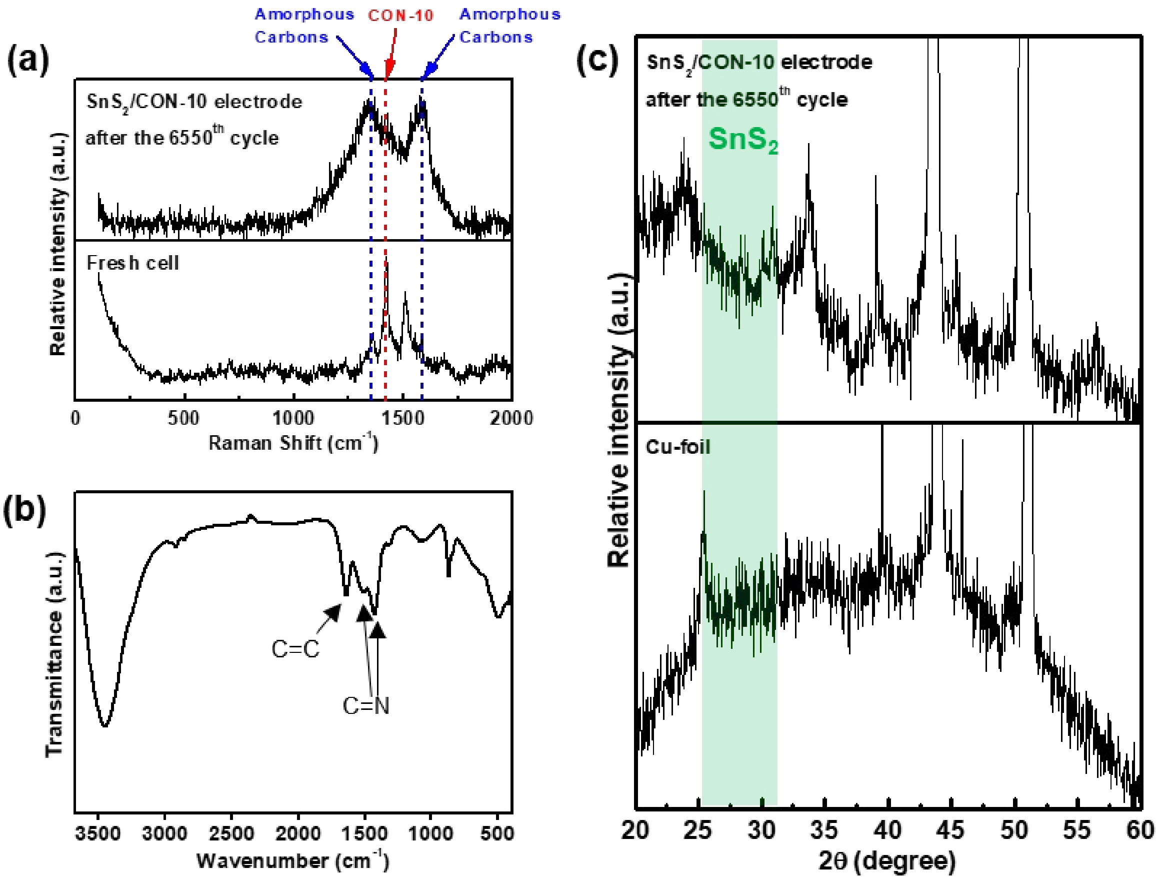

Figure S7. (a) Ex-situ FTIR profile, (b) Ex-situ Raman spectrum, and (c) XRD pattern of SnS_2/CON-10 electrodes after 6550th cycle.

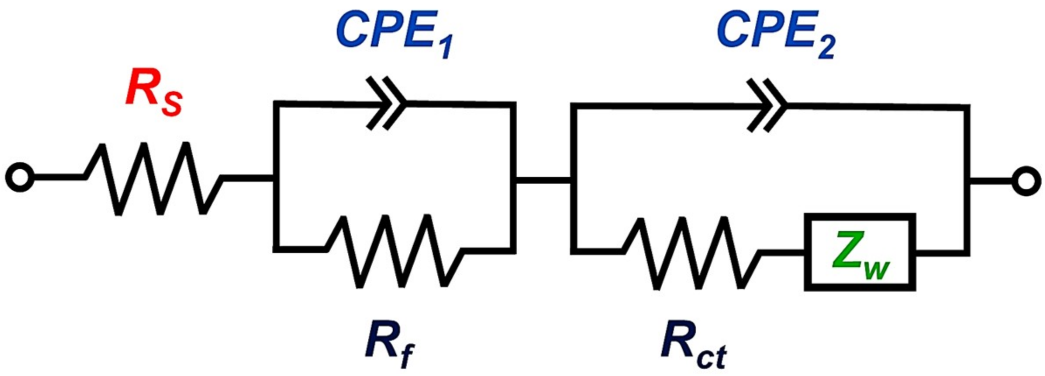

Figure S8. The equivalent circuit model for the EIS data fitting.

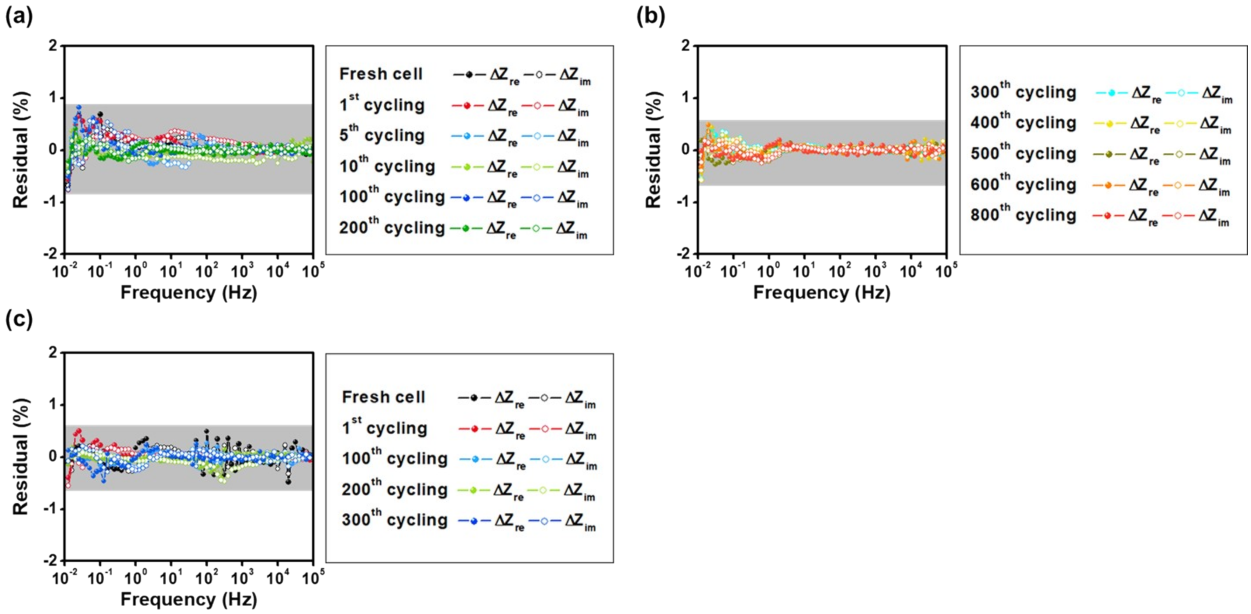

Figure S9. Relative Kramers-Kronig residuals of the (a,b) SnS_2/CON-10 and (c) as-synthesized SnS_2 electrodes.

Table S1. Summary of recent works for the SnS_2-based carbonaceous anode materials used in lithium ion batteries; ^{a}capacity (mAh/g); ^{b}cuurent density (mA/g)

Anode materials	Capacity (Capacity^{a}/Current density^{b}/Cycle number)	Voltage range (vs. Li/Li^{+})	Ref.
SnS_2/rGO-I	215.3/10/200	0.005-3	2
SnS_2@GNS	798.6/0.5/100	0.01-3	3
SnS_2/NC-5	398.9/0.1/50	0.01-3	4
SnS_2/NC@GO	603/0.1/50	0.01-3	5
hierachical SnS_2-rGO microsphere	1177.2/1/400	0.01-3	6
PPy@SnS_2@N3DG	1050/0.5/500	0.01-3	7
SnS_2/graphene multilayers	160/2/2000	0.02-3	8
SnS_2/C-NB	660.2/1/200	0.01-3	9
SnS_2/C-rGO	952/0.1/90	0.01-3	10
SnS_2-1@rGO	1045.8/0.5/700	0.05-3	11
SnS_2@g-C_3N_4	1305.7/0.5/600	0.01-3	12
SnS_2/CNTs	660/0.1/100	0.001-3	13
SnS_2/C	847.9/0.1/100	0.01-3	14
SnS_2-CNT-CC	879/2/200	0.3-3	15
SnS_2/S-rGO	1776.4/1/200	0.01-3	16
SnS_2 QDs/NG	754.2/0.5/1000	0.001-3	17
D-SnS_2/PC	596.5/1/1000	1-2.5	18
SnS_2@HMCNS	601/1/1000	0.001-3	19
SnS_2/rGO heterostructure	450/1/1000	0.02-3	20
SnS_2/CON-10	917.4/0.3/400 514.8/1/3000	0.01-3	This work

Table S2. Impedance parameters are fitted through the equivalent circuit model in **Figure S8**.

	SnS$_2$/CON-10		
	R_s (Ω)	R_f (Ω)	R_{ct} (Ω)
Fresh cell	26.4	-	71.4
1st cycling	13.9	3.51	11.8
5th cycling	12.7	4.23	18.5
10th cycling	19.7	4.59	21.6
100th cycling	20.5	4.62	32.8
200th cycling	17.2	4.68	35.3
300th cycling	17.0	3.75	33.4
400th cycling	7.3	3.59	29.8
500th cycling	13.2	3.11	24.2
600th cycling	12.9	3.28	22.7
800th cycling	13.1	3.22	21.0

The equivalent series resistance, R_s, is related to the ionic conductivity of the electrolyte and the electronic contact resistance associated with the entire cell component. The resistive element in the mid-frequency region (100 kHz to 200 mHz) appears as two resistive elements superimposed and can be identified as the film resistance (R_f) and the charge transfer resistance (R_{ct}). R_f is related to the charge transfer resistance in the solid electrolyte interface (SEI) layer and the formation of interfacial electronic contact between the current collector and the active material. R_{ct} is related to the charge transfer resistance at the interface between the electrolyte and active material.[21-26]

Table S3. Impedance parameters are fitted through the equivalent circuit model in **Figure S8**.

	as-synthesized SnS$_2$		
	R_s (Ω)	R_f (Ω)	R_{ct} (Ω)
Fresh cell	5.64	-	50.1
1st cycling	7.2	7.32	10.2
100th cycling	35.3	7.13	77.5
200th cycling	35.5	7.15	85.1
300th cycling	14.3	7.12	100.7

References

1 (a) T. Momma, N. Shiraishi, A. Yoshizawa, T. Osaka, A. Gedanken, J. Zhu, L. Sominski, *J. Power Sources*, 2001, **97–98**, 198.; H. Mukaibo, A. Yoshizawa, T. Momma, T. Osaka, *J. Power Sources*, 2003, **119–121**, 60.; M. M. Elidrissi, C. Bousquet, J. Olivier-Fourcade, C. Jumas, *Chem. Mater.*, 1998, **10**, 968.; (b) L. M. Zhu, A. W. Lei, Y. L. Cao, X. P. Ai, H. X. Yang, *Chem. Commun.* 2013, **49**, 567.; Y. Yang, C. Wang, B. Yue, S. Gambhir, C. O. Too, G. G. Wallace, *Adv. Energy Mater.*, 2012, **2**, 266.; L. Zhu, Y. Niu, Y. Cao, A. Lei, X. Ai, H. Yang, *Electrochim. Acta*, 2012, **78**, 27.; C. Zhang, Y. He, P. Mu, X. Wang, Q. He, Y. Chen, J. Zeng, F. Wang, Y. Xu, J.-X. Jiang, *Adv. Funct. Mater.*, 2018, **28**, 1705432.; (c) A. Zhu, L. Qiao, Z. Jia, P. Tan, Y. Liu, Y. Ma and J. Pan, *Dalton Trans.*, 2017, **46**, 17032–17040.

2 J. Ji, Z. Zhou, K. Fu, C. Cao, J. Yang, Y. Huang, J. Lin, J. Zhang, Z. Liu, Z. Guo, Y. Fang, Y. Xue and C. Tang, *J. Alloys Compd.*, 2020, **828**, 154192.

3 Y.-Q. Wu, Y. Yang, H. Pu, R.-Z. Gao, W.-J. Meng, H.-X. Yang and D.-L. Zhao, *J. Alloys Compd.*, 2020, **822**, 153686.

4 M. Zhang, C. Miao, R. Fang, R. Li, H. Mou and W. Xiao, *Ionics (Kiel)*, 2020, **26**, 3333–3341.

5 R. Li, C. Miao, L. Yu, H. Mou, M. Zhang and W. Xiao, *Solid State Ion.*, 2020, **348**, 115288.

6 C.-J. He, Y.-Q. Wang, W.-J. Meng, J. Zhang, Y. Xie, Y.-L. Hou and D.-L. Zhao, *J. Alloys Compd.*, 2021, **889**, 161648.

7 W. Wang, S. Guo, P. Zhang, J.-J. Zhou, Y. Yang, W. Wang, X. Xu, F. Chen and L. Chen, *ACS Appl. Energy Mater.*, 2021, **4**, 11101–11111.

8 J. Liu, Y. Chang, C. Chen, P. Guo, K. Sun, D. Cao, Y. Ma, D. Liu, Q. Liu, J. Liu and D. He, *Dalton Trans.*, 2021, **50**, 14884–14890.

9 Z. Zhang, L. Jiang, D. Wu, F. Liang, X. Li, Y. Rui and B. Tang, *J. Alloys Compd.*, 2021, **883**, 160834.

10 Y.-Q. Wu, Y.-S. Zhao, W.-J. Meng, Y. Xie, J. Zhang, C.-J. He and D.-L. Zhao, *Appl.*

Surf. Sci., 2021, **539**, 148283.

11 M. Cheng, Q. Hu, C. Du, J. Li, W. Liao, J. Li and X. Huang, *J. Solid State Chem.*, 2021, **296**, 122022.

12 H. Tran Huu, H. T. T. Le, T. Huong Nguyen, L. Nguyen Thi, V. Vo and W. Bin Im, *Appl. Surf. Sci.*, 2021, **549**, 149312.

13 Y. Cheng, H. Xie, L. Zhou, B. Shi, L. Guo and J. Huang, *Appl. Surf. Sci.*, 2021, **566**, 150645.

14 X. Xiao, F. Zhao, J. Liu, Z. Wang, Q. Sui and M. Tan, *Mater. Lett.*, 2021, **296**, 129877.

15 Z. Syum, B. Venugopal, A. Sabbah, T. Billo, T.-C. Chou, H.-L. Wu, L.-C. Chen and K.-H. Chen, *J. Power Sources*, 2021, **482**, 228923.

16 X.-X. Yang, C.-J. He, Y.-L. Hou, Y.-Q. Wang, M.-X. Ren, B.-Y. Lei, W.-J. Meng and D.-L. Zhao, *J. Electroanal. Chem. (Lausanne Switz)*, 2022, **904**, 115947.

17 S. Yin, Y. Wang, X. Zhang, Y. Sheng, B. Lan, C. Wei and G. Wen, *Vacuum*, 2022, **206**, 111482.

18 H. Luan, K. Liu, Y. Zhou and J. Sun, *Ionics (Kiel)*, 2022, **28**, 4997–5004.

19 L. Xu, X. Wu, J. Wang, Y. Dong, D. Wang, R. Wang, J. Han, R. Lv and M. Chen, *Adv. Mater. Interfaces*, 2022, **9**, 2201057.

20 J. Liu, Y. Chang, K. Sun, P. Guo, D. Cao, Y. Ma, D. Liu, Q. Liu, Y. Fu, J. Liu and D. He, *ACS Appl. Mater. Interfaces*, 2022, **14**, 11739–11749.

21 T. Jaumann, J. Balach, U. Langklotz, V. Sauchuk, M. Fritsch, A. Michaelis, V. Teltevskij, D. Mikhailova, S. Oswald, M. Klose, G. Stephani, R. Hauser, J. Eckert and L. Giebeler, *Energy Storage Mater.*, 2017, **6**, 26–35.

22 D. Aurbach, *J. Power Sources*, 2000, **89**, 206–218.

23 P. Vadhva, J. Hu, M. J. Johnson, R. Stocker, M. Braglia, D. J. L. Brett and A. J. E. Rettie, *ChemElectroChem*, 2021, **8**, 1930–1947.

24 M. Gaberšček, *Nat. Commun.*, 2021, **12**, 6513.

25 J. Moškon and M. Gaberšček, *Journal of Power Sources Advances*, 2021, **7**, 100047.

26 M. D. Levi, V. Dargel, Y. Shilina, D. Aurbach and I. C. Halalay, *Electrochim. Acta*, 2014, **149**, 126–135.